Applied Physics B (2023) 129:193
https://doi.org/10.1007/s00340-023-08135-3

Applied Physics B
Lasers and Optics

RESEARCH

High-fidelity and robust optomechanical state transfer based on pulse control

Shiken Lei[1] · Xiaojuan Wang[1] · Huan Li[1] · Rui Peng[2] · Biao Xiong[1]

Received: 1 August 2023 / Accepted: 22 October 2023 / Published online: 23 November 2023

Abstract
The extended lifespan of mechanical oscillator enables its utilization as a reliable medium for information storage. Optomechanical system coupling the cavity mode with mechanical oscillator is a promising device that can transfer the information from the light field to the mechanical oscillator for storage. In this paper, we propose an efficient scheme for quantum state transfer between the optical mode and mechanical oscillator by introducing pulsed coupling to an optomechanical system. By analyzing all the second-order moments, we give a general condition for the pulsed coupling that can guarantee the optomechanical state conversion stably. Then, we take a Gaussian-type pulsed coupling as an example to examine the analysis and show that the state initially prepared in optical mode can be transferred to the mechanical mode stably with high fidelity for storage. Moreover, our scheme exhibits high robustness against the thermal fluctuation of mechanical mode, as well as the variations in the control pulse.

1 Introduction

The quantum state transfer is a crucial task in quantum information processing, and has been concerned and studied in different quantum optical systems [1–3]. Cavity optomechanical system, coupling the optical fields with mechanical resonator via radiation pressure, makes it possible to leverage the advantages of both the optical mode and mechanical resonator [4–7]. Light, due to its high speed, is perfect for long-distance transmission of information, while mechanical resonator fits well for storing information because of its low dissipation rate [8–12]. Thus the optomechanical system is a promising device for transmitting and storing quantum information [13–15], where the information carried by light can be transferred into, stored in, and retrieved from a mechanical oscillator [16–18]. The state transfer in optomechanical system thereby is of great significance and has been extensively researched [19–28].

✉ Rui Peng
pengrui@mail.dlut.edu.cn

✉ Biao Xiong
bx_hbnu@163.com

[1] College of Physics and Electronic Science, Hubei Normal University, Huangshi 435002, China

[2] School of Physics, Dalian University of Technology, Dalian 116024, China

In optomechanical system, the interaction between optical mode and mechanical oscillator, under strong laser driving, can be reduced to beam-splitter type when the cavity resonates with mechanical mode within the red-sideband regime [29–33]. By such a beam-splitter type interaction, the mechanical mode and optical field swap energy to each other with sinusoidal and cosine oscillation in the closed system case when the coupling coefficient is constant [34, 35], in which case the state conversion happens periodically. Therefore, to obtain the best state conversion, the target time must be chosen precisely by beam-splitter type interaction with a constant coupling coefficient [36, 37]. Moreover, it is not conducive to storing quantum states carried by cavity fields on the oscillator since the oscillation. In order to store the state of the cavity field stably on the mechanical oscillator, the optomechanical coupling needs to be cut off quickly enough at the target time, which may be hard owing to the difficulty of turning on and off the optomechanical interaction sufficiently quickly [38, 39].

Quantum control is a technology that can use the time-varying control field to realize specific tasks, such as maximizing optomechanical entanglement [40, 41], generating non-classical states [42, 43], realizing optomechanical squeezing [44, 45], cooling [46, 47] and quantum synchronization [48]. In this paper, we aim to design a proposal for transferring quantum states stably from cavity mode to mechanical oscillator without sinusoidal and cosine

oscillation in a standard optomechanical system via quantum control method. Stimulated by the previous researches that propose to realize an efficient population transfer in two-level systems [49], as well as energy transfer from mirror to the cavity field [50], by a chirped pulse, we examine how a pulsed interaction can transfer the quantum state, instead of energy, from the cavity field to mechanical oscillator. Through analyzing all the second-order moments of the system, a general condition for stable optomechanical state transfer is derived. As an example, we choose the Gaussian-type coupling-pulse to discuss the state transfer proposal, we demonstrate that the initial state in the cavity field can be transferred to the mechanical mode gradually without oscillation. Moreover, the influences of cavity decay, mechanical damping, thermal noise on state conversion are researched. The experimental realization of pulsed coupling and influences of control errors on our proposal are discussed as well. We find that our scheme is robust against thermal fluctuations of mechanical mode and uncertainties in the control fields. Furthermore, we discuss the application of our scheme, especially on cat state generation.

This paper proceeds as follows. We shall first briefly introduce the model and give approximated solutions of motion equations in Sect. 2. In Sect. 3, the conditions for optomechanical state transfer are analyzed, and the parameters of the pulse are discussed and optimized. In Sect. 4, we numerically verify our analysis and discuss the effects of decoherence processes and control errors on the protocol. Sect. 5 discusses the applications of our scheme, especially on cat state generation. The last conclusion is given in Sect. 6. In addition, two appendices are attached to show the solution processes of Langevin equations and the equation of covariance matrix, respectively.

2 Model and solution

As shown in Fig. 1a, we consider a standard cavity optomechanical system, where a cavity field with eigenfrequency ω_c is coupled to a movable mechanical oscillator via radiation pressure. Assuming a laser with frequency ω_L driving the cavity, the Hamiltonian in the rotating frame with respect to the laser frequency ω_L is

$$\begin{aligned} H/\hbar =&\Delta_c a^\dagger a + \omega_m b^\dagger b - g a^\dagger a(b^\dagger + b) \\ &+ \Omega^*(t)a + \Omega(t)a^\dagger, \end{aligned} \tag{1}$$

where a and b represent the annihilation operators of cavity mode and mechanical mode, respectively; $\Delta_c = \omega_c - \omega_L$ is the cavity detuning frequency from the driving field; g denotes the coupling strength between mode a and b; $|\Omega(t)|$ describes the driving amplitude of the laser. Here we set $\Omega(t)$ time-varying, so as to design the time-dependent coupling in the following. Taking into account the dissipation κ, γ and corresponding noise terms a_{in}, b_{in}, the Heisenberg–Langevin equations of the system are

$$\dot{a} =(-i\Delta_c - \frac{\kappa}{2})a + iga(b^\dagger + b) - i\Omega(t) + \sqrt{\kappa}a_{\text{in}}, \tag{2}$$

$$\dot{b} =(-i\omega_m - \frac{\gamma}{2})b + iga^\dagger a + \sqrt{\gamma}b_{\text{in}}, \tag{3}$$

For strong laser driving amplitude $|\Omega(t)|$ and weak single-photon optomechanical coupling strength g, we can linearize the system by expanding operators a and b around their classical amplitude α and β, i.e., $a \to a + \alpha$, $b \to b + \beta$. The linearized motion equations for this system then read

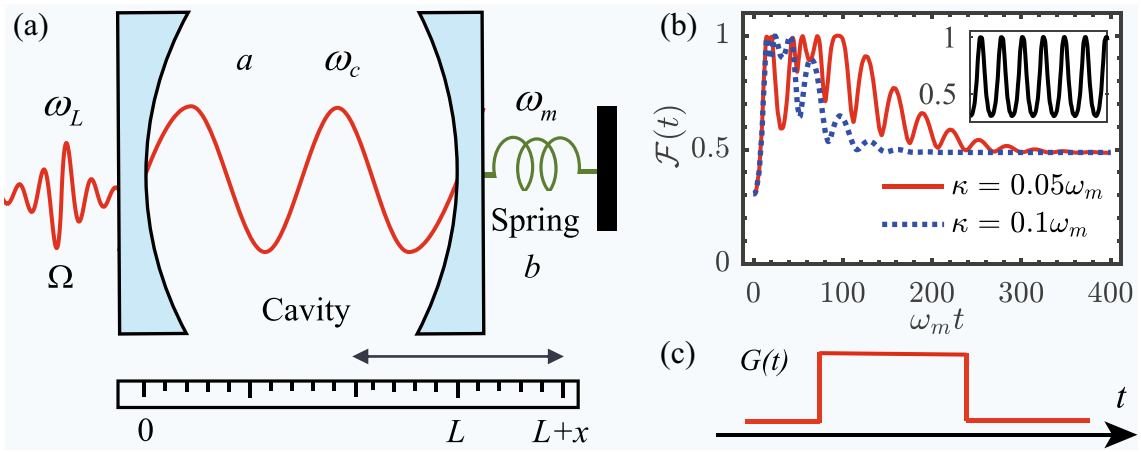

Fig. 1 Schematic of the system for state transfer. Here (a) is a standard optomechanical system with pulse modulation, and (b) shows the time evolution of fidelity of optomechanical quantum state transfer without pulse modulation, where the inset presents $\mathcal{F}(t)$ for $\kappa = 0$. (c) is the rectangular pulsed coupling that can ensure stable state transfer

$$\dot{a} = (-i\Delta - \frac{\kappa}{2})a + iG(t)(b^\dagger + b) + \sqrt{\kappa}a_{\text{in}}, \tag{4}$$

$$\dot{b} = (-i\omega_m - \frac{\gamma}{2})b + i[G^*(t)a + G(t)a^\dagger] + \sqrt{\gamma}b_{in} \tag{5}$$

when the nonlinear term is neglected under strong driving and weak coupling conditions. Here, $\Delta(t) = \Delta_c - g(\beta + \beta^*)$, $G(t) = g\alpha$, with

$$\dot{\alpha} = -i\Delta\alpha - i\Omega(t) - \frac{\kappa}{2}\alpha, \tag{6}$$

$$\dot{\beta} = -i\omega_m\beta + ig_0|\alpha|^2 - \frac{\gamma}{2}\beta. \tag{7}$$

For the thermal bath, a_{in} and b_{in} in Eqs. (4) and (5) are zero-mean Gaussian noises operators, whose correlation functions satisfy

$$\left\langle a_{\text{in}}(t)a\text{in}^\dagger(t')\right\rangle = (\bar{n}_c^{\text{th}} + 1)\delta(t - t'), \tag{8}$$

$$\left\langle b\text{in}(t)b\text{in}^\dagger(t')\right\rangle = (\bar{n}_m^{\text{th}} + 1)\delta(t - t'), \tag{9}$$

where $\bar{n}_j^{\text{th}} = \left[\exp\left(\hbar\omega_j/k_BT\right) - 1\right]^{-1}$ $(j = c, m)$ is the mean thermal excitation number from the bath. For cavity mode, $n_c^{\text{th}} \approx 0$ due to the high frequency of the optical mode. From $G(t) = g\alpha(t)$, we see that the effective coupling $G(t)$ can be controlled by modulating $\Omega(t)$ since $\alpha(t)$ is related to $\Omega(t)$. Hence, any desirable time-dependent $G(t)$ can, in principle, be achieved by adjusting the corresponding $\Omega(t)$. If the effective coupling strength $G(t)$ is constant, cavity mode and mechanical resonator will oscillate in the evolution process. To visually demonstrate this analysis, we can simulate the fidelity of state transfer from cavity to mechanical mode with Uhlmann fidelity [51]:

$$\mathcal{F}(\rho_1, \rho_2) = \left[\text{trace}\left(\sqrt{\rho_1}\rho_2\sqrt{\rho_1}\right)^{\frac{1}{2}}\right]^2, \tag{10}$$

where ρ_1 means the state to be transferred that is initially prepared in cavity mode. ρ_2 is the final state of mechanical oscillator. Without loss of generality, we assume that ρ_1 and ρ_1 are Gaussian states with the non-zero mean values $\langle a^\dagger a\rangle = 1$ and $\langle b^\dagger b\rangle = 10$ to exhibit the state transfer with constant coupling G. As shown in Fig. 1b, the quantum state transfer fidelity is oscillated with time evolution, which means the information carried in the light field will not be stably stored by the oscillator after being transferred to the oscillator. To store state in mechanical mode, the effective coupling G should turn off immediately at a fixed time when fidelity $\mathcal{F}$ reaches maximum, shown in Fig. 1c. In what follows, we propose an alternative scheme to transfer state from cavity field to mechanical mode stably by setting $G(t)$ time dependent.

In principle, $\Delta(t)$ is also time-dependent since $\Delta(t) = \Delta_c - g(\beta(t) + \beta(t)^*)$. Actually, we can modulating Δ_c with time to ensure $\Delta(t)$ time-independent [52]. To realize state conversion, we select the parameters in the red sideband regime $\Delta = \omega_m$, which can be done by PDH cavity locking technology [53]. Then we can obtain the approximate solution of Langevin equations Eqs. (4) and (5) as (see Appendix for details)

$$\begin{aligned} a(t) \approx & e^{-(i\omega_m + \frac{\kappa}{4} + \frac{\gamma}{4})t}\{\cos[h(t)]a(0) + i\sin[h(t)]b(0)\} \\ & + \int_0^t \mathrm{d}\tau' e^{-(i\omega_m + \frac{\kappa}{4} + \frac{\gamma}{4})(t-\tau')}\Big\{\sqrt{\kappa}\cos[h(t,\tau')] \\ & \times a_{\text{in}}(\tau') + i\sqrt{\gamma}\sin[h(t,\tau')]b_{\text{in}}(\tau')\Big\}, \end{aligned} \tag{11}$$

$$\begin{aligned} b(t) \approx & e^{-\left(i\omega_m + \frac{\kappa}{4} + \frac{\gamma}{4}\right)t}\{i\sin[h(t)]a(0) + \cos[h(t)]b(0)\} \\ & + \int_0^t \mathrm{d}\tau' e^{-\left(i\omega_m + \frac{\kappa}{4} + \frac{\gamma}{4}\right)(t-\tau')}\Big\{i\sqrt{\kappa}\sin[h(t,\tau')] \\ & \times a_{\text{in}}(\tau') + \sqrt{\gamma}\cos[h(t,\tau')]b_{in}(\tau')\Big\}, \end{aligned} \tag{12}$$

under the conditions of $\kappa, \gamma \ll \omega_m$, where $h(t) = \int_0^t G(\tau)\mathrm{d}\tau$ and $h(t,\tau') = \int_{\tau'}^t G(\tau)\mathrm{d}\tau$.

To find the state conversion condition, we can calculate the second-order moments or covariance matrix of cavity mode and mechanical oscillator. By Eqs. (11) and (12), we can derive the mean values of all second-order moments of the system $\bar{N}_a(t), \bar{N}_m(t), \langle a(t)a(t)\rangle, \langle b(t)b(t)\rangle, \langle a^\dagger(t)b(t)\rangle, \langle a(t)b(t)\rangle$. Here we assume that the oscillator and the cavity field are not initially correlated. Then, the mean values of second-order moments of the system are derived as

$$\begin{aligned} \langle a^\dagger(t)a(t)\rangle = & e^{-(\frac{\kappa}{2} + \frac{\gamma}{2})t}\left\{\cos^2[h(t)]\langle a^\dagger(0)a(0)\rangle\right. \\ & \left. + \sin^2[h(t)]\langle b^\dagger(0)b(0)\rangle\right\} + \int_0^t \mathrm{d}\tau' \\ & \times e^{-(\frac{\kappa}{2} + \frac{\gamma}{2})(t-\tau')}\left\{\kappa\cos^2[h(t,\tau')]\bar{n}_c^{\text{th}}\right. \\ & \left. + \gamma\sin^2[h(t,\tau')]\bar{n}_m^{\text{th}}\right\}, \end{aligned} \tag{13}$$

$$\begin{aligned} \langle b^\dagger(t)b(t)\rangle = & e^{-(\frac{\kappa}{2} + \frac{\gamma}{2})t}\left\{\sin^2[h(t)]\langle a^\dagger(0)a(0)\rangle\right. \\ & \left. + \cos^2[h(t)]\langle b^\dagger(0)b(0)\rangle\right\} + \int_0^t \mathrm{d}\tau' \\ & \times e^{-(\frac{\kappa}{2} + \frac{\gamma}{2})(t-\tau')}\left\{\kappa\sin^2[h(t,\tau')]\bar{n}_c^{\text{th}}\right. \\ & \left. + \gamma\cos^2[h(t,\tau')]\bar{n}_m^{\text{th}}\right\}, \end{aligned} \tag{14}$$

$$\begin{aligned} \langle a(t)a(t)\rangle = & e^{-(2i\omega_m + \frac{\kappa}{2} + \frac{\gamma}{2})t}\left\{\cos^2[h(t)]\langle a(0)a(0)\rangle\right. \\ & \left. - \sin^2[h(t)]\langle b(0)b(0)\right\}, \end{aligned} \tag{15}$$

$$\begin{aligned}\langle b(t)b(t)\rangle =& e^{-(2i\omega_m+\frac{\kappa}{2}+\frac{\gamma}{2})t}\Big\{-\sin^2[h(t)]\langle a^\dagger(0)a(0)\rangle \\ &+\cos^2[h(t)]\langle b^\dagger(0)b(0)\rangle\Big\},\end{aligned} \tag{16}$$

$$\begin{aligned}\langle a^\dagger(t)b(t)\rangle =& e^{-(\frac{\kappa}{2}+\frac{\gamma}{2})t}\Big\{\frac{i}{2}\sin[2h(t)](\langle a^\dagger(0)a(0)\rangle \\ &-\langle b^\dagger(0)b(0)\rangle)\Big\}+\int_0^t d\tau' e^{-(\frac{\kappa}{2}+\frac{\gamma}{2})(t-\tau')} \\ &\times\Big\{\frac{i}{2}\sin[2h(t,\tau')](\kappa\bar{n}_c^{\rm th}-\gamma\bar{n}_m^{\rm th})\Big\},\end{aligned} \tag{17}$$

$$\begin{aligned}\langle a(t)b(t)\rangle =& e^{-2(i\omega_m+\frac{\kappa}{2}+\frac{\gamma}{2})t}\Big\{\frac{i}{2}\sin[2h(t)](\langle a(0)a(0)\rangle \\ &+\langle b(0)b(0)\rangle)\Big\}.\end{aligned} \tag{18}$$

3 Analytical analysis and parameters optimization

Now, we explore what kind of time-dependent $G(t)$ can make the system transfer state stably between the cavity and mechanical oscillator. If both the diagonal and non-diagonal elements of covariance matrix for the cavity mode and oscillator are exchanged with each other through dynamical process, state conversion between cavity field and mechanical oscillator are achieved. Here, we temporarily set $\kappa=\gamma=0$ (We can also understand this condition as $\kappa << \omega_m, G$ and $\gamma << \omega_m, G$) for simplicity to analyze the result, and then discuss the influences of κ and γ on the scheme in the simulation of state transfer. Then, we can derive from Eqs. (13) to (18) that

$$\bar{N}_a(t)|_{t\to\infty}\approx\bar{N}_m(0), \tag{19}$$

$$\bar{N}_m(t)|_{t\to\infty}\approx\bar{N}_a(0), \tag{20}$$

$$\langle a^2(t)\rangle_{t\to\infty}\approx -e^{-2i\omega_m t}\langle b^2(0)\rangle, \tag{21}$$

$$\langle b^2(t)\rangle_{t\to\infty}\approx -e^{-2i\omega_m t}\langle a^2(0)\rangle, \tag{22}$$

$$\langle a^\dagger b(t)\rangle_{t\to\infty}\approx\langle ab(t)\rangle_{t\to\infty}=0, \tag{23}$$

when $h(t)$ satisfies

$$h(t)|_{t\to\infty}=\frac{\pi}{2}. \tag{24}$$

The above analysis suggests that the diagonal elements of covariance matrix for the cavity mode and oscillator can be exchanged with each other through dynamical process under the condition expressed by Eq. (24). For the non-diagonal elements, a time-dependent phase $e^{-2i\omega_m t-i\pi}$ occurs before $\langle b^2(0)\rangle$ and $\langle a^2(0)\rangle$. These time-dependent phases are vanished when we consider the state to be transferred satisfies $\langle a^2(0)\rangle=\langle b^2(0)\rangle=0$, such as vacuum state or thermal state, in which case the second-order moments of cavity mode and mechanical mode can be exchanged completely through the dynamical process. For the states, such as cat states, that $\langle a^2(0)\rangle\neq 0$ and $\langle b^2(0)\rangle\neq 0$, we will discuss it in Sect. 5 for details.

Generally speaking, there are many kinds of functions, such as Gaussian error function $\pi Erf(t)/2$, hyperbolic tangent function $\pi\tanh(t)/2$, that can satisfy the above conditions. Therefore, we can select the envelope of $G(t)$ as Gaussian pulse or hyperbolic secant pulse to meet the requirement. Without loss of generality, we choose Gaussian pulse:

$$G(t)=G_0\exp[-(t-\tau)^2/T^2], \tag{25}$$

as an example to discuss the state conversion in our system. Here G_0, τ and T are parameters to be optimized. By Eqs. (6) and (25), we can deduce that

$$\Omega(t)=\frac{ie^{\frac{-(t-\tau)^2}{T^2}}G_0(T^2(2i\Delta+\kappa)-4(t-\tau))}{2gT^2}. \tag{26}$$

Therefore, we can use the time-varying driving strength expressed above to achieve the pulsed coupling $G(t)$ shown in Eq. (25). In addition, the time-varying $\Omega(t)$ can be realized by modulating the laser power $P(t)$ with time since $|\Omega(t)|=\sqrt{P(t)\kappa/\hbar\omega_L}$. In experiments, the method of intensity modulation to the optical driving power has been employed [54]. Therefore, our pulse modulation method is technically feasible.

To optimize the Gaussian pulse expressed in Eq. (25), we simulate $|h(t)-\pi/2|$ in a long time limit in Fig. 2a, b. Figure 2a shows that τ has little effect on $|h(t)-\pi/2|$ in the long time limit for fixed T; therefore, we set $\tau=0$ to optimize the other parameters in Fig. 2b for simplicity. We see that there exits a dark blue region in Fig. 2b that $|h(t)-\pi/2|\approx 0$, which means $h(t)$ can tend to $\pi/2$ by selecting the points (G_0,T) located in the dark blue curve. In Fig. 2c, we show the time evolution of $h(t)$ by three optimized parameters pointed out in Fig. 2b, i.e., A, B, and C. It is obvious that the curves of $h(t)$ at different optimized (G_0,T) can tend to $\pi/2$ with different time scales. In Table 1, we present five sets of optimized values (τ,G_0,T).

In priciple, a larger G_0 means a shorter time costing for $h(t)$ reaching $\pi/2$, which may be useful for protecting the system from dissipation and thermal noise. However, it does not means the larger G_0, the better for the state transfer proposal since the above analyses are based on the RWA. The larger G_0, the more obvious anti-rotating-wave effect. To

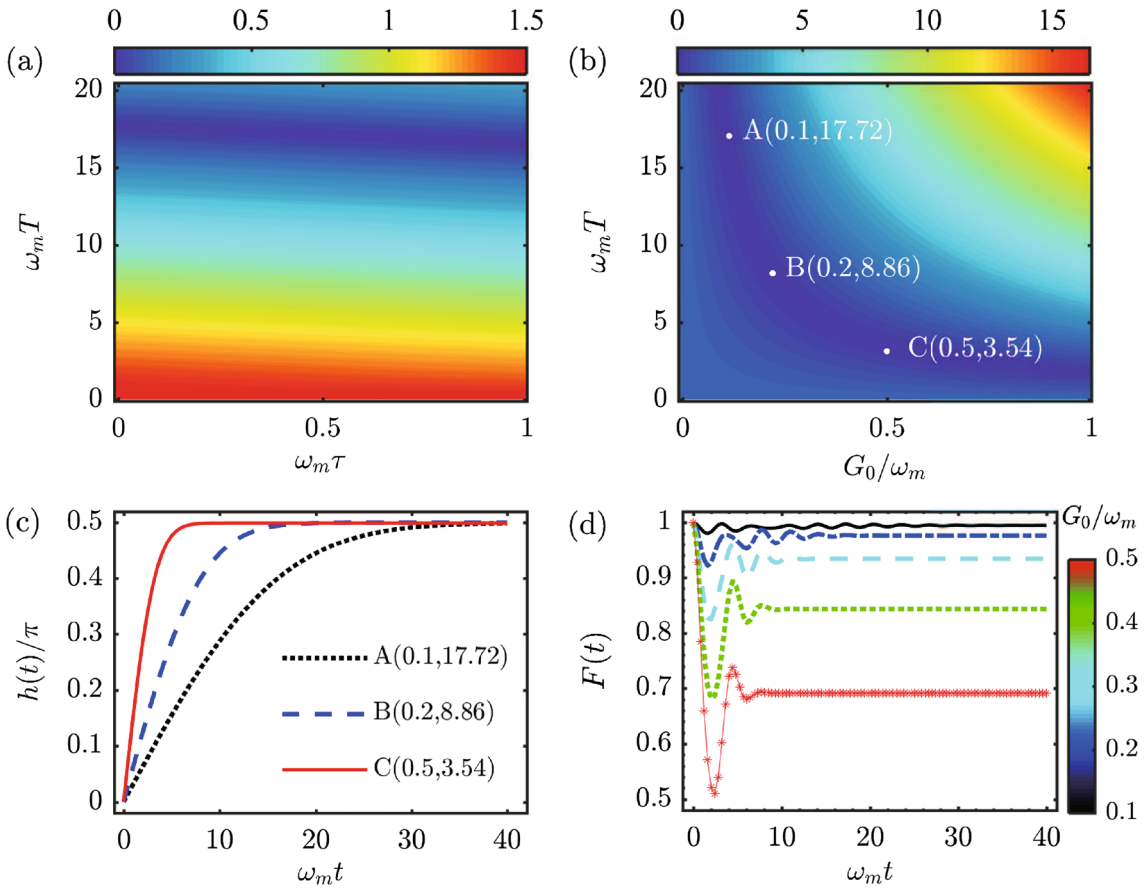

Fig. 2 Plots of $|h(t) - \pi/2|$ as functions of τ, T in (a), and G_0, T in (b) in long time limit; Time evolution of $h(t)$ in (c) for three optimized parameters pointed out (A, B, C) in (b); Time evolution of Fidelity $F(t)$. Here we set the initial state of the system as the Fock state with $\bar{N}_a(0) = 0$ and $\bar{N}_b(0) = 1$ in (d)

Table 1 Optimized values (τ, G_0, T) for the Gaussian pulse

Optimized values	$\omega_m\tau$	G_0/ω_m	$\omega_m T$
Set 1	0	0.1	17.72
Set 2	0	0.2	8.86
Set 3	0	0.3	5.91
Set 4	0	0.4	4.43
Set 5	0	0.5	3.54

examine the validity of RWA, we numerically present the time evolution of fidelity $F(t) = \left|\langle \psi_{\text{exact}}(t) \mid \psi_{\text{RWA}}(t)\rangle\right|^2$ in Fig. 2d with different optimized parameters by using Qutip [55, 56], where $|\psi_{\text{RWA}}(t)\rangle$ means the state with RWA and $|\psi_{\text{exact}}(t)\rangle$ is obtained without RWA. The results show that the fidelity $F(t)$ decreases with the increase of G_0. In the weak coupling regime, $F(t)$ is close to 1, which implies the result without RWA agrees well with that of with RWA. On the contrary, $F(t)$ is far from 1 in the strong coupling regime. In the following, we set $G_0 = 0.1\omega_m, T = 17.72/\omega_m$ to reduce the influence of anti-rotating-wave effect, so as to obtain high-fidelity optomechanical quantum state transfer.

4 Optomechanical quantum state transfer in open quantum system

To examine the above analysis, in Fig. 3, we present the time evolution of fidelity for the state transferring from cavity mode to mechanical oscillator with different kinds of initial states for mechanical mode using Uhlmann fidelity. The results show that $\mathcal{F}$ gradually increases as time evolves, and a stable fidelity as high as approximately 1.0 is reached in both Fig. 3a and b, which means the quantum state of mechanical mode both eventually becomes a vacuum state (i.e., the initial state of cavity mode), no matter whether the initial state of mechanical mode is thermal state or superposed one. In the inset of Fig. 3b, we present the dynamical trajectory in the Bloch sphere, where the red arrow describes the initial state of the oscillator $\frac{1}{\sqrt{5}}(|0\rangle + 2|1\rangle)$, the blue arrow represents the desired

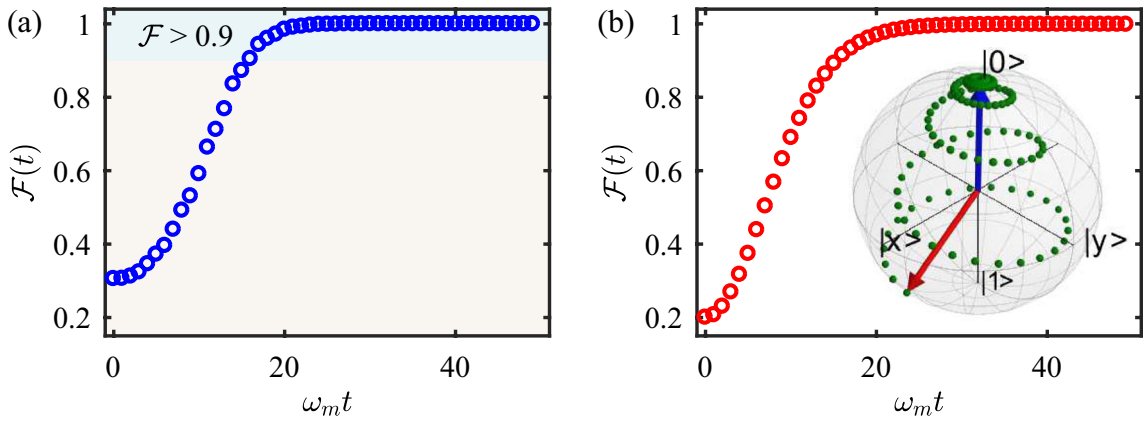

Fig. 3 Time evolution of fidelity $\mathcal{F}(t)$ for optomechanical quantum state transfer. The initial states of cavity mode and mechanical oscillator are vacuum state and thermal state with mean phonon number 10 in (a), Fock state $|0\rangle$ and superposition state $\frac{1}{\sqrt{5}}(|0\rangle + 2|1\rangle)$ in (b). The other parameters are $G_0 = 0.1\omega_m$, $T = 17.72/\omega_m$, $\kappa = 0.01\omega_m$, $\gamma = 10^{-6}\omega_m$, and $\bar{n}_m^{\text{th}} = 10$

state, which is the same as the initial state of the cavity field. Green balls in the Bloch sphere stand for quantum states at different times. It is intuitive that the state of the oscillator gradually tends to be the same as the initial state of the cavity mode as time evolution, which suggests that the state transfer is succeed.

Now, we turn to research the robustness of the state transfer protocol. If $\bar{n}_m^{\text{th}}$ is large, cutoff of the density matrix is inaccuracy. To avoid errors caused by truncation when $\bar{n}_m^{\text{th}}$ is large, it is convenient to assume the cavity mode and mechanical oscillator are both initially in Gaussian states, in which case, we can use the covariance matrix instead of density matrix for further simulation. From the Uhlmann fidelity defined by Eq. (10), one can further express the fidelity between two arbitrary Gaussian states with covariance matrix as [57–60]

$$\mathcal{F} = \frac{2}{\sqrt{\Lambda + \lambda} - \sqrt{\lambda}} \exp\left[-\xi^T \left(\widetilde{V}_1 + \widetilde{V}_2\right)^{-1} \xi\right], \tag{27}$$

where $\Lambda = \det\left(\widetilde{V}_1 + \widetilde{V}_2\right)$, $\lambda = \left(\det\widetilde{V}_1 - 1\right)\left(\det\widetilde{V}_2 - 1\right)$ and $\xi = \xi_1 - \xi_2$, with $\xi_j = (\langle X_j\rangle, \langle P_j\rangle)^T$ $(j = 1, 2)$ the column vector and $\widetilde{V}_j/2$ the corresponding covariance matrix of quantum state ρ_j. Employing Eq. (39) and (40) to Eq. (27), one can simulate precisely the protocol's fidelity for Gaussian state conversion.

In Fig. 4, we investigate the influence of cavity decay, mechanical dissipation, and thermal noise on the state transfer protocol. As shown in Fig. 4a, Fidelity $\mathcal{F}(t_f)$ decreases with the increase of the cavity decay κ and mechanical dissipation γ. Compared with cavity decay κ, mechanical dissipation γ has a greater influence on $\mathcal{F}(t_f)$. To make $\mathcal{F}(t_f) > 0.99$, γ/ω_m should be less than

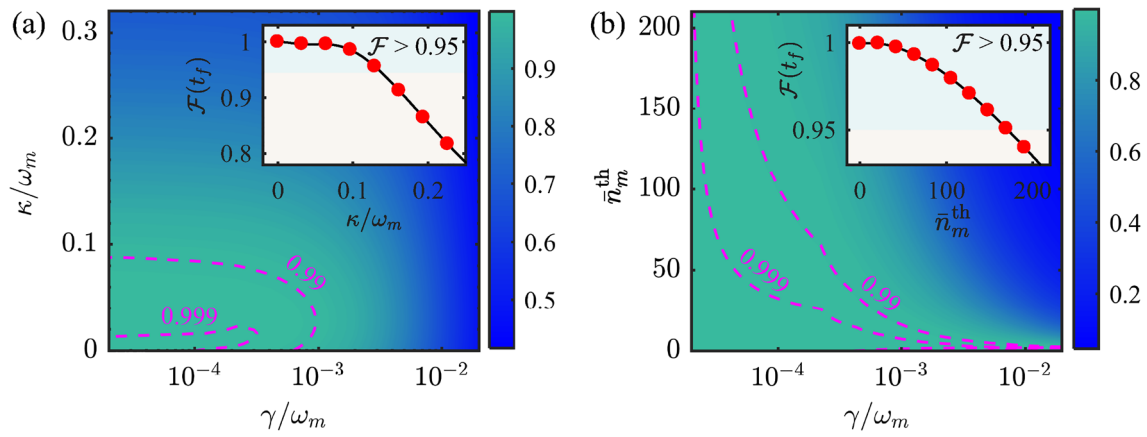

Fig. 4 Fidelity $\mathcal{F}(t_f)$ as functions of κ and γ in (a), $\bar{n}_m^{\text{th}}$ and γ in (b) at fixed time $t_f = 50/\omega_m$. We set $\gamma = 10^{-4}\omega_m$ in the inset of (a) and (b). The other parameters are the same with Fig. 3

10^{-3}. Fortunately, it is possible to achieve $\gamma/\omega_m < 10^{-3}$ in current experiments. Unlike mechanical dissipation, cavity decay seems to have less influence on $\mathcal{F}(t_f)$. When cavity decay κ/ω_m is less than 0.1, $\mathcal{F}(t_f)$ can be larger than 0.95 with appropriate mechanical dissipations, while when $\kappa/\omega_m > 0.1$, $\mathcal{F}(t_f)$ drops rapidly as κ/ω_m increases, shown in the inset of Fig. 4a, which means the state conversion scheme works well in the deeply resolved sideband regime. Although it is still challenging to achieve the deep resolved sideband regime for the cavity optomechanical system with cavity mode in optical frequency, $\kappa < \omega_m$ has been reported in electromechanical systems (i.e., optomechanical system with cavity mode in microwave frequency) [61]. Besides cavity decay and mechanical dissipation, Fig. 4b shows that the thermal excitation numbers $\bar{n}_m^{\rm th}$ harms the state conversion process. Luckily, $\mathcal{F}(t_f)$ is relatively tolerant of $\bar{n}_m^{\rm th}$. Currently, the $\bar{n}_m^{\rm th}$ reported in many experiments is less than 100 (such as $\bar{n}_m^{\rm th} \approx 57.3$ in [62], $\bar{n}_m^{\rm th} \approx 41.2$ in [63], and $\bar{n}_m^{\rm th} \approx 38.6$ in [64]). In the inset of Fig. 4b, we see that $\mathcal{F}(t_f)$ can be greater than 0.95, even when $\bar{n}_m^{\rm th}$ exceeds 100, which suggests that our scheme may be experimentally feasible.

In addition to the influences of open system, in experiments, it is also a challenge to control the waveforms of the pulse precisely. The control errors, including random noises and systematic errors, are important factors affecting the state transfer. First, we consider the influences of random noises on our state conversion protocol. For convenience, we assume that the random fluctuation satisfies the Gaussian distribution with mean value of 0 and variance of 1. Therefore, the actual pulse $\Omega_r(t)$ with random fluctuation can be written as

$$\Omega_r(t) = \Omega(t)[1 + \Gamma\mathcal{N}(0,1)], \tag{28}$$

where $\mathcal{N}(0,1)$ is a function for generating a Gaussian random number at an arbitrary time, and Γ is a constant for modulating the values of random numbers. By setting $\Gamma = 0.1$, we present the waveforms of $\Omega_r(t)$ in Fig. 5a with red line, and the corresponding time evolution of fidelity in Fig. 5b. We see that high fidelity ($\mathcal{F}(t) \simeq 0.99$ at $\omega_m t = 400$) is reached even when $\Gamma = 0.1$, which means our protocol is tolerant to classical random noises owing to the fact that random fluctuations possess random plus-minus signs, thus the time average effect of these random noises can be neglected.

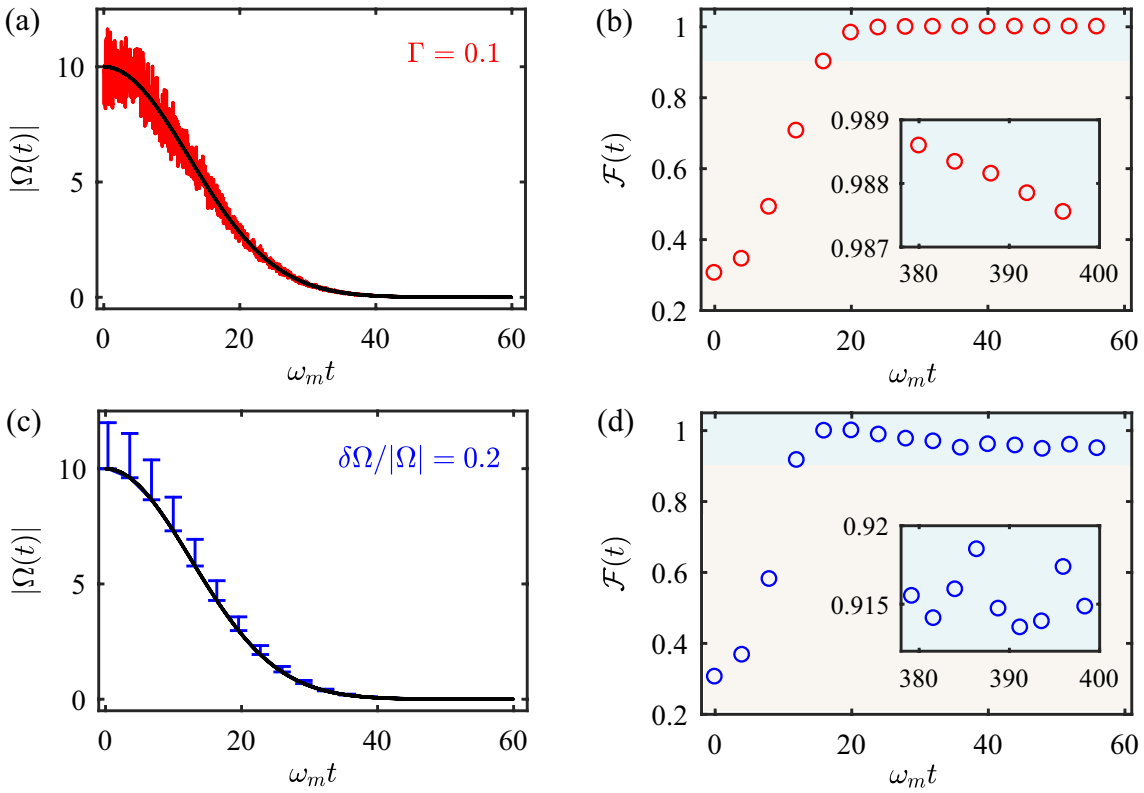

Fig. 5 (a) Waveforms of driving strength $|\Omega(t)|$ with Gaussian random noises $\Gamma\mathcal{N}(0,1)$ mixed during each time duration. (b) Time evolution of fidelity $\mathcal{F}(t)$ with $\Gamma = 0.1$. (c) Waveforms of driving strength $|\Omega(t)|$ with relative deviation $\delta\Omega/\Omega$=0.2. (d) Time evolution of fidelity $\mathcal{F}(t)$ with relative deviation $\delta\Omega/\Omega = 0.2$. We set $g = 10^{-5}\omega_m$, $\omega_m/2\pi = 2 \times 10^6$ Hz. The inset figure in (b) and (d) are the fidelity in a long time. The other parameters see Fig. 3

In addition to random noises, systematic errors induced by Ω- drifts, which may result from the imprecise apparatus and imperfect operations [65], is another factor that can influence the state transfer. Assuming that actual pulse Ω_r deviates from the ideal Ω by $\delta\Omega$, we can define the deviation as $\delta\Omega = \Omega_r - \Omega$. In Fig. 5c, the waveforms of $\Omega_r(t)$ with relative deviation $\delta\Omega/\Omega = 0.2$ are displayed with blue error bars. We see that the fidelity for state exchanging remains larger than 0.9 in a long time even when the relative deviation $\delta\Omega/\Omega = 0.2$, as shown in the inset of Fig. 5d. This result means our scheme is robust to Ω- drifts. Moreover, the fidelity $\mathcal{F}(t)$ remains larger than 0.95 for a wide time span, as displayed in Fig. 5d. Anyhow, our scheme is robust to the uncertainty of $\Omega(t)$, whether the uncertainty is caused by random noises or systematic errors. And accurately selecting the target time is not a must-do in our scheme for examining the state transfer since $\mathcal{F}(t)$ remains high with a wide time regime.

5 Discussion

In previous optomechanical systems, several works, such as double-swap protocol and adiabatic passage proposed to achieve state transfer based on a dual cavity optomechanical system. The advantage of these schemes is that the oscillator is used as a medium to achieve state transfer between fields of different frequencies. However, the double-swap protocol will suffer dissipation from all modes, including two cavities and one oscillator, and the swap time must be precisely controlled. For adiabatic state transfer schemes, the evolution of the system should not be too fast, otherwise it will be affected by intermediate mode noise and dissipation. Therefore, our solution is relatively simple and has fewer noise sources compared to state transfer in the dual cavity optomechanical system.

On the other hand, the preparation of mechanical oscillators in nonclassical states is an important topic in the field of quantum optics [66–69]. In optomechanical system, the radiation-pressure-induced interaction describes the conditional displacement process, therefore it is a good platform for generating mechanical oscillator in macroscopic Schrödinger-cat state [70]. However, the weak coupling between cavity and mechanical oscillator limits this application. It is hard to generate mechanical oscillator directly in distinguishable macroscopic Schrödinger-cat state in optomechanical system [71, 72]. Compared to mechanical mode, cavity field is a little easier to be generated in Schrödinger-cat state, and has been experimentally realized [73, 74]. Thus an alternative method to generate mechanical mode in cat state is employing state conversion protocol: First generate Schrödinger-cat state of cavity field, then transform it to mechanical mode. For the cavity mode initially prepared in a cat state, i.e., $\langle a^2(0)\rangle \neq 0$, the off-diagonal elements of covariance matrix for mechanical oscillator in long time limit will be $\langle b^2(t)\rangle_{t\to\infty} = -e^{-2i\omega_m t}\langle a^2(0)\rangle$ through the dynamical process in our scheme, which makes the obtained state at time t different from the desired state to be transferred. Actually, for the mechanical oscillator, by using Eq. (22), we can derive the relation between the desired state $|\phi_m\rangle$ and obtained state $|\psi_m\rangle$ in the long time limit as

$$|\psi_m\rangle = \exp\{-i(\omega_m t - \pi/2)b^\dagger b\}|\phi_m\rangle. \tag{29}$$

If the cavity is initially prepared in Schrödinger-cat state $N_+(|\eta\rangle + |-\eta\rangle)$, the state for mechanical mode will be

$$|\psi_m\rangle = N_+(|-ie^{-i\omega_m t}\eta\rangle + |ie^{-i\omega_m t}\eta\rangle) \tag{30}$$

in long time limit. Although the above state is different from the desired state $|\phi_m\rangle = N_+(|\eta\rangle + |-\eta\rangle)$, $|\psi_m\rangle$ is still a Schrödinger-cat state, which implies we can prepare macroscopic Schrödinger-cat state in mechanical oscillator with our scheme by first generating cavity mode in cat state. Figure 6a shows the process of cat state generation by Qutip. It is obvious that the state of mechanical mode gradually becomes a cat state from the initial thermal state, and the phase of obtained cat state is changing with time evolution. In addition, the fidelity for cat state generation of mechanical mode is high with current parameter conditions, as shown in Fig. 6b.

In addition, one of the most important tasks in the optomechanical system is to cool mechanical mode to its ground state to reduce thermal fluctuation. Sideband cooling and feedback cooling are two powerful tools that can be used to meet this goal and have been widely discussed in many previous works. Actually, the cooling process is not the only way that can achieve the ground state of the mechanical oscillator. By using the pulse modulation method discussed in this paper, the vacuum state in the cavity field can be transferred to the mechanical oscillator, which can also realize the ground state of mechanical mode. Compared with sideband cooling and feedback cooling, the pulse modulation method may be much more quick to prepare mechanical mode in its ground state because there is no oscillation in the evolutions with the pulse modulation method proposed above. And since the strong mechanical squeezing and entanglement can be realized by joining the cooling process with parametric process [75–77], the protocol may also be extended to generate mechanical squeezing by adding a parametric driving to the mechanical mode, and entanglement by adding another non-degenerate parametric interaction to the system.

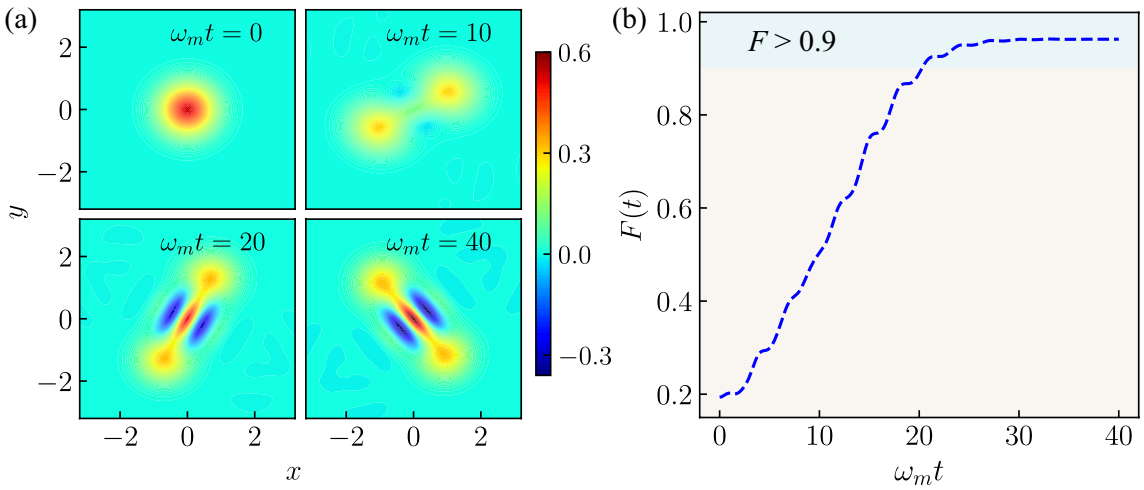

Fig. 6 (a) Wigner function of mechanical mode for different t. (b) Fidelity for cat state generation

6 Conclusion

In summary, we have proposed a robust proposal for transferring quantum states in optomechanical system. In our scheme, the pulsed coupling is introduced to the system. By analyzing the equations of all the second-order moments of the optomechanical system, we give a general condition that the pulsed coupling should satisfy for quantum state conversion. As an example, we choose the Gaussian-type pulsed coupling to discuss the state conversion from the cavity fields to the mechanical oscillator. Results show that optomechanical state transfer can be accomplished with high fidelity under the optimized parameters used in the main text. Moreover, the system will not oscillate when the state transfer is completed in our protocol, which on the one hand makes it possible for the oscillator to play the role of memory: store the quantum state stably, on the other hand makes our scheme allow a wide range of target time for detecting the stored states. Even considering the influence of cavity decay rate, mechanical dissipation, thermal noise, and error of control fields, high fidelity can be still obtained. Especially, the scheme is robust against thermal fluctuation of mechanical oscillator and variation of control field, which is experimentally friendly, and may have potential application in quantum devices such as quantum memory.

Appendix A: Approximate solutions of Langevin equation

In this appendix, we present a detailed derivation of the approximate solution $a(t)$ and $b(t)$ given in the main text (i.e., Eqs. (11) and (12)). We start from Eqs. (4) and (5). In red-detuned sideband regime $\Delta = \omega_m$, the $b^\dagger$ term in Eq. (4) and $a^\dagger$ term in Eq. (5) can be ignored due to the rotating-wave approximation (RWA), thus Eqs. (4) and (5) can be approximated as

$$\dot{a} = \left(-i\Delta - \frac{\kappa}{2}\right)a + iG(t)b + \sqrt{\kappa}a_{\mathrm{i\,n}}, \tag{31}$$

$$\dot{b} = \left(-i\omega_m - \frac{\gamma}{2}\right)b + iG(t)a + \sqrt{\gamma}b_{\mathrm{in}}, \tag{32}$$

where we have chosen the phase reference of the classical driving field to ensure that $G(t)$ is real. To solve Eqs. (31) and (32), we rewrite it in the compact form

$$\frac{\mathrm{d}}{\mathrm{d}t}\psi_0(t) = \mathcal{A}_0\psi_0(t) + \psi_{0,\mathrm{in}}(t), \tag{33}$$

for simplicity, where $\psi_0 = (a, b)^T, \psi_{0,\mathrm{in}} = (\sqrt{\kappa}a_{\mathrm{in}}, \sqrt{\gamma}b_{\mathrm{in}})^T$, and

$$A_0 = \begin{pmatrix} -i\Delta - \frac{\kappa}{2} & iG(t) \\ iG(t) & -i\omega_m - \frac{\gamma}{2} \end{pmatrix}. \tag{34}$$

One of the general methods to solve the matrix differential equation is to diagonalize the coefficient matrix A_0. However, the eigenstates of the coefficient matrix contain $G(t)$. Since $G(t)$ is assumed to be time-dependent, the above equation is hard to be solved accurately. Here, we consider the scheme worked in deep-resolved-sideband regime $\kappa \ll \omega_m$, in which case, we can neglect κ and γ temporarily, thus the eigenmodes of the coefficient matrix A_0 are

$$\psi_1 = \frac{1}{\sqrt{2}}(-1, 1)^T, \quad \psi_2 = \frac{1}{\sqrt{2}}(1, 1)^T, \tag{35}$$

Then, we can define the quasi-mode A and B by transform $(A, B)^T = S(a, b)^T$, where $S = (\psi_1, \psi_2) = \frac{1}{\sqrt{2}}\begin{pmatrix} -1 & 1 \\ 1 & 1 \end{pmatrix}$.

Therefore, the Langevin equations Eq. (33) can be expressed with quasi-mode A and B as

$$\frac{\mathrm{d}}{\mathrm{d}t}\widetilde{\psi}_0(t) = \widetilde{\mathcal{A}}_0\widetilde{\psi}_0(t) + \widetilde{\psi}_{0,\mathrm{in}}(t), \tag{36}$$

where $\widetilde{\psi}_0 = (A, B)^T$, $\widetilde{\psi}_{0,\mathrm{in}} = (A_{\mathrm{in}}, B_{\mathrm{in}})$, and

$$\widetilde{\mathcal{A}}_0 = \begin{pmatrix} -i\left(\omega_m + G(t)\right) - \frac{\kappa}{4} - \frac{\gamma}{4}, & \frac{\kappa}{4} - \frac{\gamma}{4} \\ \frac{\kappa}{4} - \frac{\gamma}{4}, & i\left(G(t) - \omega_m\right) - \frac{\kappa}{4} - \frac{\gamma}{4} \end{pmatrix}.$$

Here $Ain = (\sqrt{\gamma}b\mathrm{in} - \sqrt{\kappa}a\mathrm{in})/\sqrt{2}$ and $Bin = (\sqrt{\gamma}b\mathrm{in} + \sqrt{\kappa}a\mathrm{in})/\sqrt{2}$. Under the condition of $\kappa, \gamma \ll \omega_m$, we can ignore the off-diagonal elements of the coefficient matrix, in which case, the differential equations of A and B are decoupled, and we can get

$$A(t) \approx e^{-(i\omega_m + \frac{\kappa}{4} + \frac{\gamma}{4})t - i\int_0^t G(\tau)\mathrm{d}\tau} A(0) + \int_0^t \mathrm{d}\tau' A_{\mathrm{in}}(\tau') e^{-(i\omega_m + \frac{\kappa}{4} + \frac{\gamma}{4})(t-\tau') - i\int_{\tau'}^t G(\tau)\mathrm{d}\tau},$$

$$B(t) \approx e^{-(i\omega_m + \frac{\kappa}{4} + \frac{\gamma}{4})t + i\int_0^t G(\tau)\mathrm{d}\tau} B(0) + \int_0^t \mathrm{d}\tau' B_{\mathrm{in}}(\tau') e^{-(i\omega_m + \frac{\kappa}{4} + \frac{\gamma}{4})(t-\tau') + i\int_{\tau'}^t G(\tau)\mathrm{d}\tau}.$$

By applying the inverse unitary transform $(a, b)^T = S^{-1}(A, B)^T$, we can obtain the final expression of a and b in the main text (see Eqs. (11) and (12)).

Appendix B: Equation of Covariance matrix

To give the equation of covariance matrix, we first write Eqs. (4), (5) and their Hermite conjugate in the compact form as

$$\frac{\mathrm{d}}{\mathrm{d}t}\psi(t) = \mathcal{A}\psi(t) + \psi_{\mathrm{in}}(t) \tag{37}$$

by introducing $\psi = (a, a^\dagger, b, b^\dagger)^T$, $\psi_{\mathrm{in}} = \left(\sqrt{\kappa}a_{\mathrm{in}}, \sqrt{\kappa}a^\dagger_{\mathrm{in}}, \sqrt{\gamma}b_{\mathrm{in}}, \sqrt{\gamma}b^\dagger_{\mathrm{in}}\right)^T$, and

$$\mathcal{A} = \begin{pmatrix} -i\Delta - \frac{\kappa}{2} & 0 & iG(t) & iG(t) \\ [6pt]0 & i\Delta - \frac{\kappa}{2} & -iG(t) & -iG(t) \\ [6pt]iG(t) & iG(t) & -i\omega_m - \frac{\gamma}{2} & 0 \\ [6pt]-iG(t) & -iG(t) & 0 & i\omega_m - \frac{\gamma}{2} \end{pmatrix}. \tag{38}$$

For the linearized system, the dynamics can be completely characterized by the covariance matrix V, whose element is defined as $V_{ij} = \left\langle \psi_i\psi_j + \psi_j\psi_i \right\rangle/2$. According to Eq. (37), one can obtain

$$\frac{\mathrm{d}}{\mathrm{d}t}V = \mathcal{A}V + V\mathcal{A}^T + D \tag{39}$$

by a simple derivation, where $D = \mathrm{diag}\left(D_c, D_m\right)$ with $D_c = \kappa\sigma_x/2$, and $D_m = \gamma\left(\bar{n}_m^{\mathrm{th}} + 1/2\right)\sigma_x$ (σ_x is the Pauli matrix). By introducing $X_c = (a + a^\dagger)/\sqrt{2}$, $P_c = (a - a^\dagger)/\sqrt{2}i$, $X_m = (b + b^\dagger)/\sqrt{2}$ and $P_m = (b - b^\dagger)/\sqrt{2}i$, the covariance matrix $\widetilde{V}$ defined as $\widetilde{V}_{ij} = \left\langle O_iO_j + O_jO_i \right\rangle/2$ ($O = (X_c, P_c, X_m, P_m)^T$) can be expressed as

$$\widetilde{V} = RVR^T, \tag{40}$$

where $R = \mathrm{diag}\left(R_1, R_2\right)$ with $R_j = \frac{1}{\sqrt{2}}\begin{pmatrix} 1 & 1 \\ -i & i \end{pmatrix}$.

Acknowledgements We thank Ms. Binbin Zhang for valuable suggestions on writing. This work was supported by the National Natural Science Foundation of China (Grant No. 12104141).

Author contributions SL performed the main analytical calculations and wrote the main manuscript. XW conceived the idea, designed the research, and performed the simulations HL prepared figures. RP and BX analyzed the results, provided critical insights, and polished the writing. All authors reviewed the manuscript

Data availability Data will be made available on request.

Declarations

Conflict of interest The authors declare no competing interests

References

1. C. Kurz, M. Schug, P. Eich, J. Huwer, P. Müller, J. Eschner, Experimental protocol for high-fidelity heralded photon-to-atom quantum state transfer. Nat. Commun. **5**(1), 5527 (2014). https://doi.org/10.1038/ncomms6527
2. F. Mei, G. Chen, L. Tian, S.-L. Zhu, S. Jia, Robust quantum state transfer via topological edge states in superconducting qubit chains. Phys. Rev. A **98**, 012331 (2018). https://doi.org/10.1103/PhysRevA.98.012331
3. X.-M. Zhang, Z. Wei, R. Asad, X.-C. Yang, X. Wang, When does reinforcement learning stand out in quantum control? a comparative study on state preparation. NPJ Quantum Inf. **5**(1), 85 (2019). https://doi.org/10.1038/s41534-019-0201-8
4. M. Aspelmeyer, T.J. Kippenberg, F. Marquardt, Cavity optomechanics. Rev. Mod. Phys. **86**, 1391–1452 (2014). https://doi.org/10.1103/RevModPhys.86.1391
5. X. Zhao, Macroscopic entanglement in optomechanical system induced by non-markovian environment. Opt. Express **27**(20), 29082–29097 (2019). https://doi.org/10.1364/OE.27.029082
6. Y. Wei, X. Wang, B. Xiong, C. Zhao, J. Liu, C. Shan, Improving few-photon optomechanical effects with coherent feedback. Opt. Express **29**(22), 35299–35313 (2021). https://doi.org/10.1364/OE.440382

7. B. Xiong, S. Chao, C. Shan, J. Liu, Optomechanical squeezing with pulse modulation. Opt. Lett. **47**(21), 5545–5548 (2022). https://doi.org/10.1364/OL.471230
8. V. Fiore, Y. Yang, M.C. Kuzyk, R. Barbour, L. Tian, H. Wang, Storing optical information as a mechanical excitation in a silica optomechanical resonator. Phys. Rev. Lett. **107**, 133601 (2011). https://doi.org/10.1103/PhysRevLett.107.133601
9. B. Li, P.-B. Li, Y. Zhou, S.-L. Ma, F.-L. Li, Quantum microwave-optical interface with nitrogen-vacancy centers in diamond. Phys. Rev. A **96**, 032342 (2017). https://doi.org/10.1103/PhysRevA.96.032342
10. D.P. Lake, M. Mitchell, D.D. Sukachev, P.E. Barclay, Processing light with an optically tunable mechanical memory. Nat. Commun. **12**(1), 663 (2021). https://doi.org/10.1038/s41467-021-20899-w
11. M. Pechal, P. Arrangoiz-Arriola, A.H. Safavi-Naeini, Superconducting circuit quantum computing with nanomechanical resonators as storage. Quantum Sci. Technol. **4**(1), 015006 (2018). https://doi.org/10.1088/2058-9565/aadc6c
12. M.-S. Ding, Y. Shi, Y.-J. Liu, L. Zheng, Magnon control of light transmission in a symmetric-like cavity magnomechanical system. Physica Scripta **97**(9), 095104 (2022)
13. M.J. Weaver, F. Buters, F. Luna, H. Eerkens, K. Heeck, S. Man, D. Bouwmeester, Coherent optomechanical state transfer between disparate mechanical resonators. Nat. Commun. **8**(1), 824 (2017). https://doi.org/10.1038/s41467-017-00968-9
14. E.A. Sete, H. Eleuch, High-efficiency quantum state transfer and quantum memory using a mechanical oscillator. Phys. Rev. A **91**, 032309 (2015). https://doi.org/10.1103/PhysRevA.91.032309
15. D. Mansouri, B. Rezaie, N. Ranjbar, A. Daeichian, Optomechanical cavity-atom interaction through field coupling in a composed quantum system: a filtering approach. Appl. Phys. B **129**(4), 58 (2023)
16. S.A. McGee, D. Meiser, C.A. Regal, K.W. Lehnert, M.J. Holland, Mechanical resonators for storage and transfer of electrical and optical quantum states. Phys. Rev. A **87**, 053818 (2013). https://doi.org/10.1103/PhysRevA.87.053818
17. R.Y. Teh, S. Kiesewetter, M.D. Reid, P.D. Drummond, Simulation of an optomechanical quantum memory in the nonlinear regime. Phys. Rev. A **96**, 013854 (2017). https://doi.org/10.1103/PhysRevA.96.013854
18. R.Y. Teh, S. Kiesewetter, P.D. Drummond, M.D. Reid, Creation, storage, and retrieval of an optomechanical cat state. Phys. Rev. A **98**, 063814 (2018). https://doi.org/10.1103/PhysRevA.98.063814
19. Y.-D. Wang, A.A. Clerk, Using interference for high fidelity quantum state transfer in optomechanics. Phys. Rev. Lett. **108**, 153603 (2012). https://doi.org/10.1103/PhysRevLett.108.153603
20. L. Tian, Adiabatic state conversion and pulse transmission in optomechanical systems. Phys. Rev. Lett. **108**, 153604 (2012). https://doi.org/10.1103/PhysRevLett.108.153604
21. F.-Y. Zhang, W.-L. Li, W.-B. Yan, Y. Xia, Speeding up adiabatic state conversion in optomechanical systems. J. Phys. B At. Mol. Opt. Phys. **52**(11), 115501 (2019). https://doi.org/10.1088/1361-6455/ab08d8
22. C. Ventura-Velázquez, B. Jaramillo Ávila, E. Kyoseva, B.M. Rodríguez-Lara, Robust optomechanical state transfer under composite phase driving. Sci. Rep. **9**(1), 4382 (2019). https://doi.org/10.1038/s41598-019-40492-y
23. M.-A. Lemonde, V. Peano, P. Rabl, D.G. Angelakis, Quantum state transfer via acoustic edge states in a 2d optomechanical array. New J. Phys. **21**(11), 113030 (2019). https://doi.org/10.1088/1367-2630/ab51f5
24. L. Qi, G.-L. Wang, S. Liu, S. Zhang, H.-F. Wang, Controllable photonic and phononic topological state transfers in a small optomechanical lattice. Opt. Lett. **45**(7), 2018–2021 (2020). https://doi.org/10.1364/OL.388835
25. H. Molinares, V. Eremeev, M. Orszag. Steady-state squeezing transfer in hybrid optomechanics. In: *Frontiers in Optics+Laser Science 2021* (Optica Publishing Group, 2021), , pp. 1–83. https://doi.org/10.1364/FIO.2021.JTu1A.83. http://opg.optica.org/abstract.cfm?URI=FiO-2021-JTu1A.83
26. J.M. Fink, M. Kalaee, R. Norte, A. Pitanti, O. Painter, Efficient microwave frequency conversion mediated by a photonics compatible silicon nitride nanobeam oscillator. Quantum Sci. Technol. **5**(3), 034011 (2020). https://doi.org/10.1088/2058-9565/ab8dce
27. L. Liu, B.-P. Hou, X.-H. Zhao, B. Tang, Squeezing transfer of light in a two-mode optomechanical system. Opt. Express **27**(6), 8361–8374 (2019). https://doi.org/10.1364/OE.27.008361
28. C. Genes, A. Mari, D. Vitali, P. Tombesi. Chapter 2 quantum effects in optomechanical systems. In *Advances in Atomic Molecular and Optical Physics. Advances In Atomic, Molecular, and Optical Physics*, vol. 57 (Academic Press, 2009), pp. 33–86. https://doi.org/10.1016/S1049-250X(09)57002-4. https://www.sciencedirect.com/science/article/pii/S1049250X09570024
29. Y.-C. Liu, Y.-F. Xiao, X. Luan, C.W. Wong, Dynamic dissipative cooling of a mechanical resonator in strong coupling optomechanics. Phys. Rev. Lett. **110**, 153606 (2013). https://doi.org/10.1103/PhysRevLett.110.153606
30. W.P. Bowen, G.J. Milburn, *Quantum Optomechanics* (CRC Press, Boca Raton, 2015)
31. S. Barzanjeh, A. Xuereb, S. Gröblacher, M. Paternostro, C.A. Regal, E.M. Weig, Optomechanics for quantum technologies. Nat. Phys. **18**(1), 15–24 (2022). https://doi.org/10.1038/s41567-021-01402-0
32. S.-L. Chao, Z. Yang, C.-S. Zhao, R. Peng, L. Zhou, Force sensing in a dual-mode optomechanical system with linear-quadratic coupling and modulated photon hopping. Opt. Lett. **46**(13), 3075–3078 (2021). https://doi.org/10.1364/OL.425484
33. N. Benrass, D. Aoune, N. Habiballah, M. Nassik, Quantification of different quantum correlations in a double cavity optomechanical system. Mod. Phys. Lett. A **37**(01), 2250007 (2022). https://doi.org/10.1142/S0217732322500079
34. L. Tian, H. Wang, Optical wavelength conversion of quantum states with optomechanics. Phys. Rev. A **82**, 053806 (2010). https://doi.org/10.1103/PhysRevA.82.053806
35. J. Cheng, X.-T. Liang, W.-Z. Zhang, X. Duan, Optomechanical state transfer in the presence of non-markovian environments. Opt. Commun. **430**, 385–390 (2019). https://doi.org/10.1016/j.optcom.2018.08.079
36. G.D. Moraes Neto, F.M. Andrade, V. Montenegro, S. Bose, Quantum state transfer in optomechanical arrays. Phys. Rev. A **93**, 062339 (2016). https://doi.org/10.1103/PhysRevA.93.062339
37. Y.-X. Zeng, J. Shen, M.-S. Ding, C. Li, Macroscopic schrödinger cat state swapping in optomechanical system. Opt. Express **28**(7), 9587–9602 (2020). https://doi.org/10.1364/OE.385814
38. T. Palomaki, J. Harlow, J. Teufel, R. Simmonds, K.W. Lehnert, Coherent state transfer between itinerant microwave fields and a mechanical oscillator. Nature **495**(7440), 210–214 (2013)
39. N. Lilienfein, S. Holzberger, I. Pupeza. In *Ultrafast Optomechanical Pulse Picking*, ed. by D. Meschede, T. Udem, T. Esslinger (Springer, Cham, 2018), pp. 371–387. https://doi.org/10.1007/978-3-319-64346-5_21
40. D. Stefanatos, Maximising optomechanical entanglement with optimal control. Quantum Sci. Technol. **2**(1), 014003 (2017). https://doi.org/10.1088/2058-9565/aa629c

41. S.G. Hofer, W. Wieczorek, M. Aspelmeyer, K. Hammerer, Quantum entanglement and teleportation in pulsed cavity optomechanics. Phys. Rev. A **84**, 052327 (2011). https://doi.org/10.1103/PhysRevA.84.052327
42. Y.-H. Chen, W. Qin, X. Wang, A. Miranowicz, F. Nori, Shortcuts to adiabaticity for the quantum rabi model: efficient generation of giant entangled cat states via parametric amplification. Phys. Rev. Lett. **126**, 023602 (2021). https://doi.org/10.1103/PhysRevLett.126.023602
43. V. Bergholm, W. Wieczorek, T. Schulte-Herbrüggen, M. Keyl, Optimal control of hybrid optomechanical systems for generating non-classical states of mechanical motion. Quantum Sci. Technol. **4**(3), 034001 (2019). https://doi.org/10.1088/2058-9565/ab1682
44. B. Xiong, X. Li, S.-L. Chao, Z. Yang, W.-Z. Zhang, W. Zhang, L. Zhou, Strong mechanical squeezing in an optomechanical system based on lyapunov control. Photon. Res. **8**(2), 151–159 (2020). https://doi.org/10.1364/PRJ.8.000151
45. D.-Y. Wang, C.-H. Bai, S. Liu, S. Zhang, H.-F. Wang, Dissipative bosonic squeezing via frequency modulation and its application in optomechanics. Opt. Express **28**(20), 28942–28953 (2020). https://doi.org/10.1364/OE.399687
46. C.-H. Bai, D.-Y. Wang, S. Zhang, S. Liu, H.-F. Wang, Double-mechanical-oscillator cooling by breaking the restrictions of quantum backaction and frequency ratio via dynamical modulation. Phys. Rev. A **103**, 033508 (2021). https://doi.org/10.1103/PhysRevA.103.033508
47. Z. Yang, J. Yang, S.-L. Chao, C. Zhao, R. Peng, L. Zhou, Simultaneous ground-state cooling of identical mechanical oscillators by lyapunov control. Opt. Express **30**(11), 20135–20148 (2022). https://doi.org/10.1364/OE.460646
48. W. Li, C. Li, H. Song, Quantum synchronization in an optomechanical system based on lyapunov control. Phys. Rev. E **93**, 062221 (2016). https://doi.org/10.1103/PhysRevE.93.062221
49. L. Allen, J.H. Eberly, *Optical Resonance and Two-level Atoms*, vol. 28 (Courier Corporation, Chelmsford, 1987)
50. J.-Q. Liao, C.K. Law, Cooling of a mirror in cavity optomechanics with a chirped pulse. Phys. Rev. A **84**, 053838 (2011). https://doi.org/10.1103/PhysRevA.84.053838
51. A. Uhlmann, The "transition probability'' in the state space of a*-algebra. Rep. Math. Phys. **9**(2), 273–279 (1976)
52. B. Xiong, X. Li, S.-L. Chao, L. Zhou, Optomechanical quadrature squeezing in the non-markovian regime. Opt. Lett. **43**(24), 6053–6056 (2018). https://doi.org/10.1364/OL.43.006053
53. R.W.P. Drever, J.L. Hall, F.V. Kowalski, J. Hough, G.M. Ford, A.J. Munley, H. Ward, Laser phase and frequency stabilization using an optical resonator. Appl. Phys. B **31**(2), 97–105 (1983). https://doi.org/10.1007/BF00702605
54. C.C. Rodrigues, C.M. Kersul, A.G. Primo, M. Lipson, T.P. Alegre, G.S. Wiederhecker, Optomechanical synchronization across multi-octaves frequency spans. arXiv:2105.01791 (2021)
55. J.R. Johansson, P.D. Nation, F. Nori, Qutip: an open-source python framework for the dynamics of open quantum systems. Comput. Phys. Commun. **183**(8), 1760–1772 (2012). https://doi.org/10.1016/j.cpc.2012.02.021
56. J.R. Johansson, P.D. Nation, F. Nori, Qutip 2: a python framework for the dynamics of open quantum systems. Comput. Phys. Commun. **184**(4), 1234–1240 (2013). https://doi.org/10.1016/j.cpc.2012.11.019
57. B.D. Clader, Quantum networking of microwave photons using optical fibers. Phys. Rev. A **90**, 012324 (2014). https://doi.org/10.1103/PhysRevA.90.012324
58. H. Scutaru, Fidelity for displaced squeezed thermal states and the oscillator semigroup. J. Phys. A Math. Gen. **31**(15), 3659–3663 (1998). https://doi.org/10.1088/0305-4470/31/15/025
59. A. Isar, Quantum fidelity of gaussian states in open systems. Phys. Part. Nucl. Lett. **6**(7), 567–571 (2009)
60. W. Li, C. Li, H. Song, Quantum synchronization and quantum state sharing in an irregular complex network. Phys. Rev. E **95**, 022204 (2017). https://doi.org/10.1103/PhysRevE.95.022204
61. C.U. Lei, A.J. Weinstein, J. Suh, E.E. Wollman, A. Kronwald, F. Marquardt, A.A. Clerk, K.C. Schwab, Quantum nondemolition measurement of a quantum squeezed state beyond the 3 db limit. Phys. Rev. Lett. **117**, 100801 (2016). https://doi.org/10.1103/PhysRevLett.117.100801
62. E.E. Wollman, C.U. Lei, A.J. Weinstein, J. Suh, A. Kronwald, F. Marquardt, A.A. Clerk, K.C. Schwab, Quantum squeezing of motion in a mechanical resonator. Science **349**(6251), 952–955 (2015). https://doi.org/10.1126/science.aac5138
63. F. Lecocq, J.B. Clark, R.W. Simmonds, J. Aumentado, J.D. Teufel, Mechanically mediated microwave frequency conversion in the quantum regime. Phys. Rev. Lett. **116**, 043601 (2016). https://doi.org/10.1103/PhysRevLett.116.043601
64. L.D. Tóth, N.R. Bernier, A. Nunnenkamp, A.K. Feofanov, T.J. Kippenberg, A dissipative quantum reservoir for microwave light using a mechanical oscillator. Nat. Phys. **13**(8), 787–793 (2017). https://doi.org/10.1038/nphys4121
65. J.-L. Wu, Y. Wang, J. Song, Y. Xia, S.-L. Su, Y.-Y. Jiang, Robust and highly efficient discrimination of chiral molecules through three-mode parallel paths. Phys. Rev. A **100**, 043413 (2019). https://doi.org/10.1103/PhysRevA.100.043413
66. F. Xue, Y.-X. Liu, C.P. Sun, F. Nori, Two-mode squeezed states and entangled states of two mechanical resonators. Phys. Rev. B **76**, 064305 (2007). https://doi.org/10.1103/PhysRevB.76.064305
67. J.R. Johansson, N. Lambert, I. Mahboob, H. Yamaguchi, F. Nori, Entangled-state generation and bell inequality violations in nanomechanical resonators. Phys. Rev. B **90**, 174307 (2014). https://doi.org/10.1103/PhysRevB.90.174307
68. W. Qin, A. Miranowicz, H. Jing, F. Nori, Generating long-lived macroscopically distinct superposition states in atomic ensembles. Phys. Rev. Lett. **127**, 093602 (2021). https://doi.org/10.1103/PhysRevLett.127.093602
69. F.-Y. Zhang, C.-P. Yang, Generation of generalized hybrid entanglement in cavity electro–optic systems. Quantum Sci. Technol. **6**(2), 025003 (2021). https://doi.org/10.1088/2058-9565/abd221
70. W. Marshall, C. Simon, R. Penrose, D. Bouwmeester, Towards quantum superpositions of a mirror. Phys. Rev. Lett. **91**, 130401 (2003). https://doi.org/10.1103/PhysRevLett.91.130401
71. J.-Q. Liao, L. Tian, Macroscopic quantum superposition in cavity optomechanics. Phys. Rev. Lett. **116**, 163602 (2016). https://doi.org/10.1103/PhysRevLett.116.163602
72. J. Clarke, M.R. Vanner, Growing macroscopic superposition states via cavity quantum optomechanics. Quantum Sci. Technol. **4**(1), 014003 (2018). https://doi.org/10.1088/2058-9565/aada1d
73. A. Ourjoumtsev, H. Jeong, R. Tualle-Brouri, P. Grangier, Generation of optical 'schrödinger cats' from photon number states. Nature **448**(7155), 784–786 (2007)
74. B. Hacker, S. Welte, S. Daiss, A. Shaukat, S. Ritter, L. Li, G. Rempe, Deterministic creation of entangled atom-light schrödinger-cat states. Nat. Photon. **13**(2), 110–115 (2019)
75. A. Kronwald, F. Marquardt, A.A. Clerk, Arbitrarily large steady-state bosonic squeezing via dissipation. Phys. Rev. A **88**, 063833 (2013). https://doi.org/10.1103/PhysRevA.88.063833

76. X.-Y. Lü, J.-Q. Liao, L. Tian, F. Nori, Steady-state mechanical squeezing in an optomechanical system via duffing nonlinearity. Phys. Rev. A **91**, 013834 (2015). https://doi.org/10.1103/PhysRevA.91.013834
77. Y.-D. Wang, A.A. Clerk, Reservoir-engineered entanglement in optomechanical systems. Phys. Rev. Lett. **110**, 253601 (2013). https://doi.org/10.1103/PhysRevLett.110.253601